Familial pulmonary alveolar proteinosis caused by mutations in *CSF2RA*

Takuji Suzuki,[1] Takuro Sakagami,[1] Bruce K. Rubin,[5] Lawrence M. Nogee,[6] Robert E. Wood,[2] Sarah L. Zimmerman,[3] Teresa Smolarek,[3] Megan K. Dishop,[7] Susan E. Wert,[1] Jeffrey A. Whitsett,[1] Gregory Grabowski,[3] Brenna C. Carey,[1] Carrie Stevens,[4] Johannes C.M. van der Loo,[4] and Bruce C. Trapnell[1,2,8]

[1]Division of Pulmonary Biology, [2]Division of Pulmonary Medicine, [3]Division of Human Genetics, and [4]Division of Experimental Hematology and Cancer Biology, Cincinnati Children's Hospital Medical Center, Cincinnati, OH 45229
[5]Departments of Pediatrics and Biomedical Engineering, Wake Forest University School of Medicine, Winston-Salem, NC 27157
[6]Department of Pediatrics, Johns Hopkins University, Baltimore, MD 21205
[7]Department of Pathology, Texas Children's Hospital, Houston, TX 77030
[8]Division of Pulmonary, Critical Care, and Sleep Medicine, Department of Medicine, University of Cincinnati College of Medicine, Cincinnati, OH 45267

Primary pulmonary alveolar proteinosis (PAP) is a rare syndrome characterized by accumulation of surfactant in the lungs that is presumed to be mediated by disruption of granulocyte/macrophage colony-stimulating factor (GM-CSF) signaling based on studies in genetically modified mice. The effects of GM-CSF are mediated by heterologous receptors composed of GM-CSF binding (GM-CSF-Rα) and nonbinding affinity-enhancing (GM-CSF-Rβ) subunits. We describe PAP, failure to thrive, and increased GM-CSF levels in two sisters aged 6 and 8 yr with abnormalities of both GM-CSF-Rα–encoding alleles (*CSF2RA*). One was a 1.6-Mb deletion in the pseudoautosomal region of one maternal X chromosome encompassing *CSF2RA*. The other, a point mutation in the paternal X chromosome allele encoding a G174R substitution, altered an N-linked glycosylation site within the cytokine binding domain and glycosylation of GM-CSF-Rα, severely reducing GM-CSF binding, receptor signaling, and GM-CSF–dependent functions in primary myeloid cells. Transfection of cloned cDNAs faithfully reproduced the signaling defect at physiological GM-CSF concentrations. Interestingly, at high GM-CSF concentrations similar to those observed in the index patient, signaling was partially rescued, thereby providing a molecular explanation for the slow progression of disease in these children. These results establish that GM-CSF signaling is critical for surfactant homeostasis in humans and demonstrate that mutations in *CSF2RA* cause familial PAP.

CORRESPONDENCE
Bruce C. Trapnell:
Bruce.Trapnell@cchmc.org

Pulmonary surfactant homeostasis is maintained by the balanced production of surfactant by alveolar epithelium and its clearance by pulmonary alveolar macrophages (1). GM-CSF is a critical regulator of surfactant homeostasis in mice (1). GM-CSF, via heterologous cell surface receptors comprised of α and β glycoprotein subunits (GM-CSF-Rα and GM-CSF-Rβ, respectively), activates STAT5 and other signaling pathways (2). N-linked glycosylation of the α subunit is required for GM-CSF binding and receptor signaling (3). In mice, deficiency of GM-CSF (4, 5) or its receptor (6) impairs multiple functions of alveolar macrophages (7), including surfactant catabolism (8), which results in progressive surfactant accumulation.

Pulmonary alveolar proteinosis (PAP) is a syndrome characterized by respiratory failure caused by pulmonary surfactant accumulation (9, 10), which can be grouped into distinct categories based on clinical, histopathologic, biochemical, and genetic data (1, 9–12). Primary PAP occurs when GM-CSF signaling is disrupted, for example in individuals with high levels of GM-CSF autoantibodies, which are

The online version of this article contains supplemental material.

Supplemental material can be found at:
http://doi.org/10.1084/jem.20080990

presumed to mediate pathogenesis by neutralizing GM-CSF and reducing surfactant catabolism by alveolar macrophages (10, 13). This form, referred to as autoimmune PAP, comprises 90% of cases (13). Primary PAP has also been associated with reduced detection of GM-CSF-Rβ on myeloid cells (14, 15), but definitive studies demonstrating heritable deficiency of either GM-CSF or its receptors as the cause of PAP in humans are lacking (16). Secondary PAP occurs as a consequence of an underlying disease presumed to impair surfactant clearance by reducing either the numbers or functions of alveolar macrophages (9). Hereditary disorders of surfactant production, for example, because of mutations in the genes encoding surfactant protein (SP)–B (17), SP-C (18), or ABCA3 (19), exhibit disordered surfactant homeostasis to varying degrees but are distinguished from PAP by their surfactant dysfunction, disruption of alveolar wall architecture, and clinical course (20). In this paper, we describe a family in which two children developed primary PAP in association with loss of GM-CSF responsiveness caused by mutations in the gene encoding GM-CSF-Rα.

RESULTS AND DISCUSSION

Clinical presentation and phenotype

The index patient presented at age six with a 2-yr history of progressive tachypnea and failure to thrive (height and weight were third percentile for age [Fig. S1 A, available at http://www.jem.org/cgi/content/full/jem.20080990/DC1]). Gestation, delivery, birth weight (3.66 kg, 50th percentile), and development were all normal, but weight gain slowed by 6–9 mo as did height by 2–3 yr. There was no history of cough, fever, chest pain, pneumonia or other pulmonary disease, environmental exposure, or drug use. Both parents were well-developed and healthy with no history of lung disease. Examination revealed moderate tachypnea, mild tachycardia, and inspiratory crackles but was otherwise unremarkable. Pulmonary function testing revealed severe restrictive impairment. Oxygen saturation was 88% while breathing room air and decreased while talking or walking a short distance. A diagnosis of PAP was suspected based on chest radiography (Fig. 1 A) and established by histopathologic examination of lung tissue (Fig. 1 B). A serum GM-CSF autoantibody test (21) was negative on two occasions. The patient was transferred to Cincinnati Children's Hospital and underwent whole lung lavage therapy with marked symptomatic and radiographical improvement (Fig. 1 C). MCP-1 and M-CSF levels in the lavage were increased compared with healthy controls (supplemental text, available at http://www.jem.org/cgi/content/full/jem.20080990/DC1), which is similar to findings in autoimmune PAP patients and GM-CSF KO mice (22, 23).

An inherited defect in GM-CSF receptor function was suspected based on the constellation of histopathology showing well-preserved alveolar wall architecture (Fig. 1 B), the absence of GM-CSF autoantibodies (21), and an abnormal CD11b stimulation index test (24). Therefore, all immediate family members were evaluated. Because SP is in serum in PAP and levels reflect lung disease severity (25), serum SP-D

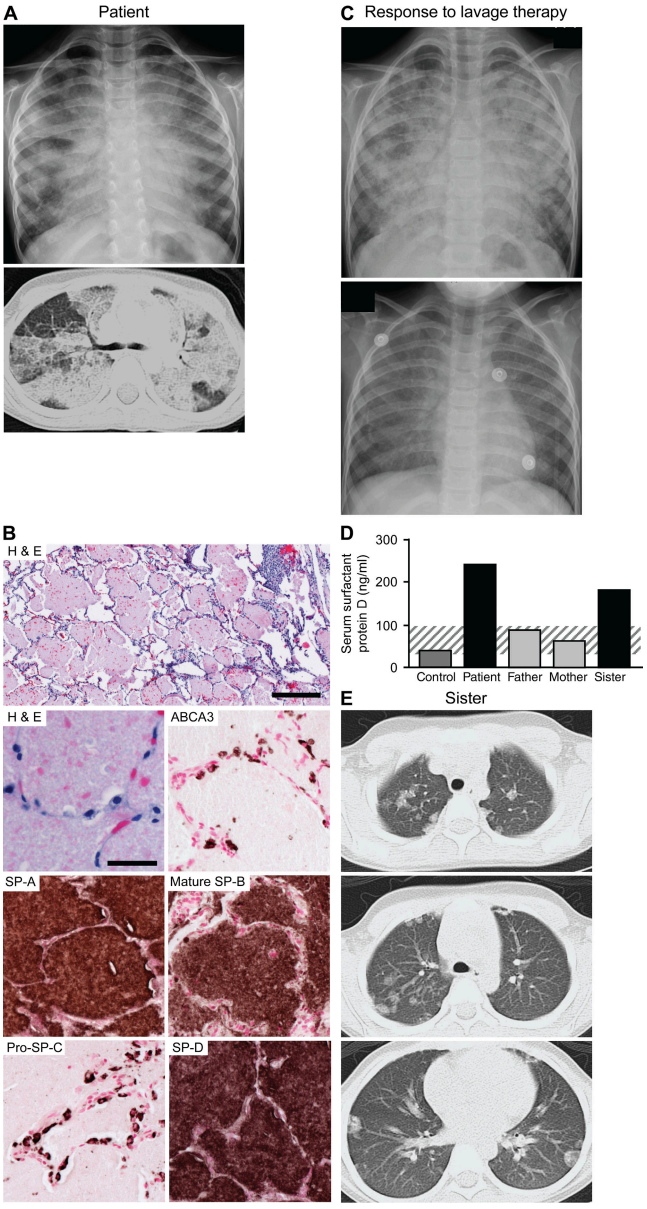

Figure 1. Phenotypic characterization of patients with familial PAP. (A) Chest radiograph (top) and high-resolution computed tomogram of the chest (bottom) of the index patient at presentation. (B) Histopathologic appearance of the open lung biopsy from the index patient after staining with hematoxylin and eosin (H&E) or immunostaining for SP-A, mature SP-B, Pro–SP-C, SP-D, and ABCA3. Note the lymphocytosis in the low-power hematoxylin and eosin–stained section and the intact alveolar wall in the high-powered hematoxylin and eosin–stained section. Images were obtained at a total magnification of 50× (top) or 400× (all others). Bars: (top) 100 μm; (all others) 10 μm. (C) Chest radiograph of the index patient 4 mo after presentation immediately before (top) and 5 d after (bottom) whole lung lavage therapy. (D) Serum SP-D levels in affected siblings, parents, and a control. The mean ± SD serum SP-D concentration in 67 healthy controls was 63.5 ± 39 ng/ml (hatched region) and in 12 patients with autoimmune PAP was 174 ± 83 ng/ml (not indicated). (E) High-resolution computed tomogram showing diffuse patchy ground glass opacities representing mild PAP in the affected sister.

was measured and found to be increased in the patient compared with her parents and controls (Fig. 1 D). Unexpectedly, the patient's 8-yr-old sister, who was previously thought to be healthy, had increased serum SP-D. Subsequent clinical evaluation revealed that the sister had poor growth (height and weight, 10th percentile for age; Fig. S1B), a diffusion capacity for carbon dioxide of 57% that predicted, and mild patchy ground glass opacities throughout both lungs, which are consistent with a diagnosis of PAP (Fig. 1 E).

Structure and function of the GM-CSF receptor

Flow cytometry indicated that GM-CSF-Rα and GM-CSF-Rβ were present on blood leukocytes in all family members (Fig. 2 A). Western blotting revealed an abnormal electrophoretic pattern for GM-CSF-Rα in the patient and her sister with predominantly lower molecular mass forms compared with the control (Fig. 2 B). The father was heterozygous for normal and lower molecular mass forms. Unexpectedly, the mother exhibited only a normal pattern. To evaluate cell-mediated clearance of GM-CSF, blood mononuclear cells from the patient (Fig. 2 C) and her sister (Fig. S2, available at http://www.jem.org/cgi/content/full/jem.20080990/DC1) were incubated with GM-CSF, and both failed to clear GM-CSF in contrast to control and parental leukocytes. The concentration of GM-CSF in lung lavage was markedly increased in the patient compared with healthy controls, in whom it was undetectable (Fig. 2 D). The in vivo concentration of pulmonary GM-CSF in the epithelial lining fluid of the lungs was estimated to be 6.9 and 27 ng/ml (right and left lungs, respectively) using the urea dilution method (26). Pulmonary

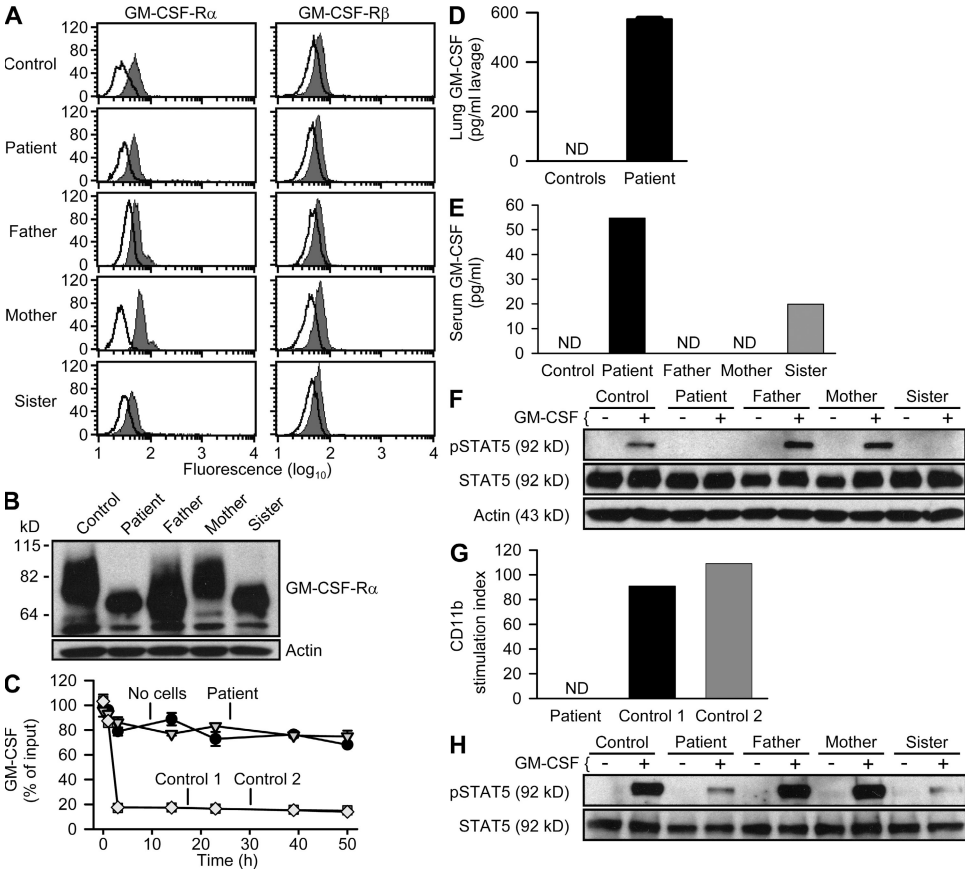

Figure 2. Structural and functional analysis of GM-CSF receptor defects. (A) Flow cytometry demonstrating GM-CSF-Rα and GM-CSF-Rβ on the cell surface of peripheral blood leukocytes in all family members. (B) Western blots of PBMC lysates using antibodies to detect GM-CSF-Rα or actin as indicated. (C) GM-CSF clearance assay. Blood leukocytes from the patient were unable to remove exogenous GM-CSF added to culture medium at time zero in contrast to leukocytes from two controls that rapidly bound and cleared GM-CSF. Error bars show the means ± SE. (D and E) Measurement of GM-CSF concentration by ELISA. GM-CSF was readily detected in lavage from the patient but was not detected (ND) in lung lavage from nine healthy controls (D). GM-CSF was detected in the serum of affected siblings but not their parents or a control (E). (F) Blood leukocytes isolated from the indicated family members were incubated for 15 min in the absence (−) or presence (+) of 10 ng/ml GM-CSF, followed by Western blotting of cell lysates to detect total STAT5 (STAT5), phosphorylated STAT5 (pSTAT5), or actin. (G) Measurement of the GM-CSF–stimulated increase in CD11b levels on leukocytes in whole blood. The CD11b stimulation index (24) was calculated as the mean fluorescence of CD11b on leukocytes incubated with GM-CSF minus that of unstimulated cells divided by that of unstimulated cells and multiplied by 100. (H) Similar to F except that a higher GM-CSF concentration (1,000 ng/ml) was used and cell lysates were immunoprecipitated with anti-STAT5 antibody before Western blotting to detect total STAT5 (STAT5) or phosphorylated STAT5 (pSTAT5).

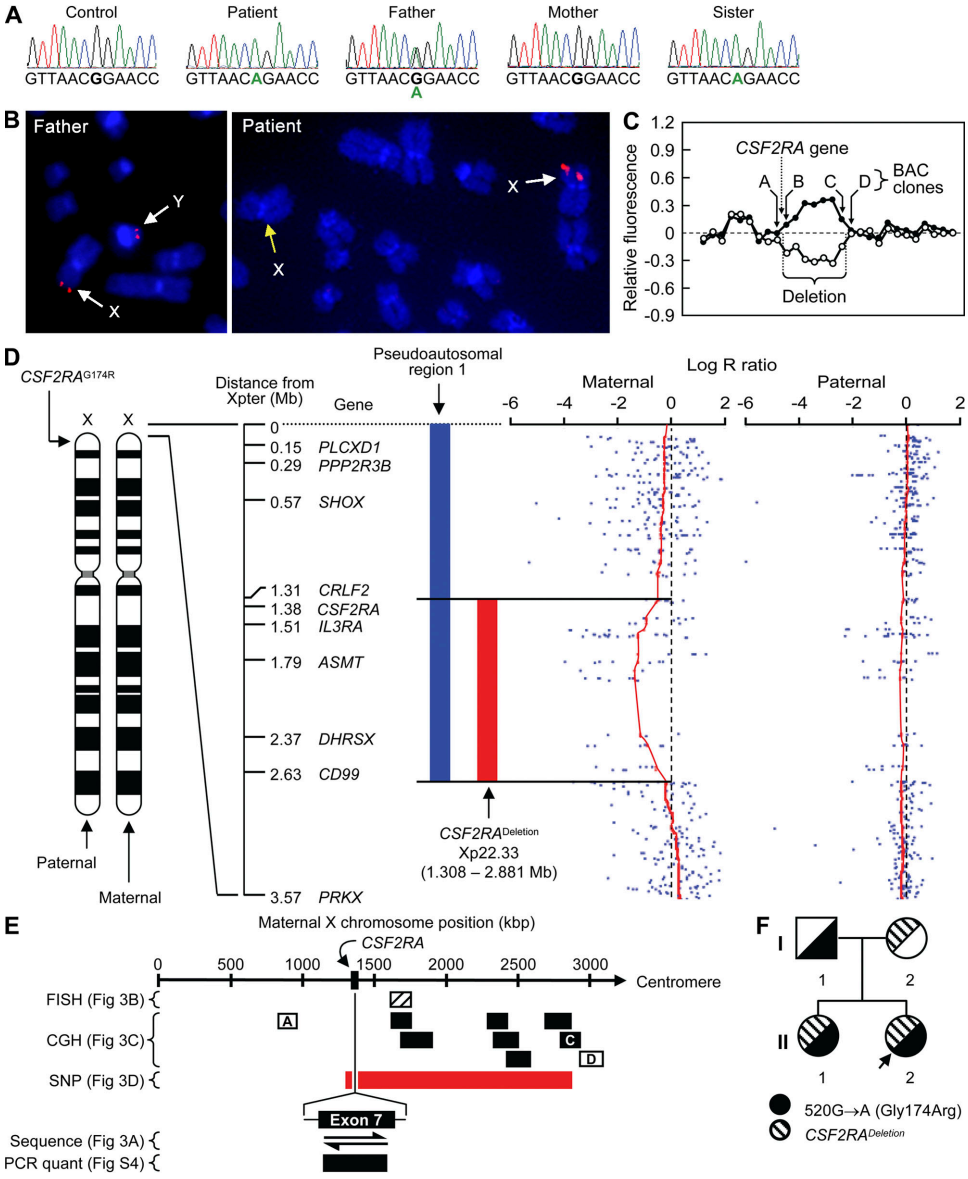

Figure 3. Genetic analysis of *CSF2RA* gene defects. (A) Nucleotide sequence of *CSF2RA* in genomic DNA from each family member, including nt 580–591 of the coding sequence (numbered relative to the initiation codon; from GenBank/EMBL/DDBJ under accession no. NM_006140.3). The index patient and her sister exhibited only a G→A point mutation at nt 586. The father was heterozygous for this substitution and the mother exhibited only the normal sequence. (B) FISH analysis to detect *CSF2RA* sequences in genomic DNA from the father and the patient. The probe (CTD-3047L21), which maps to the pseudoautosomal region (Xp22.33 and Yp11.32), hybridized to both X and Y chromosomes in the father (white arrows) and to one (white arrow), but not the other (yellow arrow), X chromosome in the patient. 8–10 metaphase cells and 25 interphase cells were evaluated for each individual. Similar FISH analyses are shown for each family member in the supplemental material (available at http://www.jem.org/cgi/content/full/jem.20080990/DC1). Images were obtained at a total magnification of 1000×. (C) CGH analysis for the patient in the region of Xp22.33. The relative fluorescence of fluorescently labeled DNA from the patient (open circles) compared with a same-sex reference DNA (filled circles) after hybridization to various BAC clones on the SignatureSelect V2 chip representing the Xp22.33 region is shown. Reduced hybridization to several BAC clones (clones B and C) is indicated by the lower fluorescence of the patient's DNA compared with the reference DNA for these BAC clones. The telomeric breakpoint is mapped to between clones A and B and the centromeric breakpoint is mapped to between clones C and D. These data indicate an interstitial deletion of ∼1.264 Mb at Xp22.33 encompassing ∼1,610,183–2,873,864 bp. The dashed line represents a relative fluorescence of zero. (D) High-resolution SNP mapping of the Xp22 region for paternal and maternal X chromosomes. A schematic shows the locations of the point mutation (*CSF2RA*^{G174R}) in the paternal X chromosome and the 1.6-Mb deletion at Xp22.33 in the maternal X chromosome and the genes encompassed. The base 2 ratio of normalized hybridization intensities for patient and reference samples (log R ratio) is shown. Similar SNP analyses for each family member are shown in the supplemental material (available at http://www.jem.org/cgi/content/full/jem.20080990/DC1). (E) Map showing a portion of the X chromosome summarizing the genetic analysis used to identify the small maternal X chromosomal deletion at Xp22.33 encompassing *CSF2RA*. The probe used for FISH analysis (hatched bar) is the same as clone B on the CGH microarray chip. The locations of selected CGH microarray probes in the region of the CSF2RA gene are shown. Those CGH probes showing

GM-CSF was also increased in *CSF2RB*-deficient mice (Fig. S3), confirming the relationship between GM-CSF receptor dysfunction and increased pulmonary GM-CSF levels. Serum GM-CSF was increased in both affected siblings and undetectable in both parents and control, indicating that the abnormality was systemic (Fig. 2 E). GM-CSF receptor function was impaired in both affected siblings, as shown by reduced GM-CSF–stimulated phosphorylation of STAT5 (Fig. 2 F) and failure of GM-CSF to increase CD11b levels on leukocytes from the patient compared with controls (Fig. 2 G).

The slower-than-expected rate of progression of PAP in both affected siblings led us to hypothesize that the GM-CSF-Rα abnormality may not completely abolish GM-CSF signaling. This was confirmed by incubation of primary blood mononuclear cells with a higher concentration of GM-CSF (1,000 ng/ml), which resulted in partial receptor signaling as shown by an increase in phosphorylated STAT5 (Fig. 2 H). Thus, although both GM-CSF-Rα and β chains were present on leukocytes in all family members, in the two affected siblings, the GM-CSF-Rα chain was structurally abnormal, which severely reduced but did not completely abolish GM-CSF binding and GM-CSF–dependent signaling and cellular functions.

Genetic analysis of the GM-CSF receptor

The nucleotide sequence of the *CSF2RA* gene in genomic DNA from both siblings revealed a single G→A point mutation in exon 7 that encoded a nonconservative amino acid change (glycine to arginine) at position 174, G174R (Fig. 3 A). This change alters one of the 11 potential sites of N-glycosylation, which is required for GM-CSF receptor function (3, 27). The father was heterozygous for mutant $CSF2RA^{G174R}$ and WT ($CSF2RA^{WT}$) alleles (Fig. 3 A), whereas only the $CSF2RA^{WT}$ sequence was detected in the mother (Fig. 3 A). The sequence of *CSF2RA* in leukocyte messenger RNA (mRNA) was similar to the respective DNA sequence for each family member, even when cDNA was overamplified to detect potentially underrepresented mRNA sequences (unpublished data). This absence of a normal sequence for *CSF2RA* exon 7 in both siblings and the absence of the point mutation in the mother suggested that one maternal *CSF2RA* allele may be deleted in the patient, her sister, and their mother. The nucleotide sequence of *CSF2RB* in leukocyte mRNA from all family members was normal (unpublished data).

PCR amplification demonstrated a reduced copy number of *CSF2RA* in genomic DNA from both siblings and their mother compared with the father and a healthy control (Fig. S4, available at http://www.jem.org/cgi/content/full/jem.20080990/DC1). In contrast, the genomic copy number of *CSF2RB* was similar in all family members and a control (Fig. S4). Routine cytogenetic analysis was normal in all family members (Fig. S5), ruling out a large chromosomal abnormality. Fluorescent in situ hybridization (FISH) demonstrated a deletion in the pseudoautosomal region 1 of the X chromosome in the patient (Fig. 3 B), her sister, and mother (Fig. S6) that was not present in the father (Fig. 3 B). Further evaluation using comparative genomic hybridization (CGH) demonstrated an interstitial deletion encompassing the region from ∼1,610,183 to 2,873,864 bp on one maternal-derived X chromosome in the patient (Fig. 3 C), her sister, and mother (not depicted). High-resolution single-nucleotide polymorphism (SNP) mapping further defined this small deletion as extending from 1,308,324 to 2,881,011 bp in one maternal X chromosome (Fig. 3 D) and in both siblings (Fig. S7). Importantly, this deletion encompassed the *CSF2RA* allele (Fig. 3 E), thereby explaining the unexpected *CSF2RA* DNA and mRNA sequence results.

These results demonstrate the inheritance of compound heterozygous abnormalities of *CSF2RA* in both siblings (Fig. 3 F). The G174R mutation present on the paternal X chromosome, localized to the extracellular cytokine binding domain of GM-CSF-Rα, alters a potential site of glycosylation and impairs GM-CSF binding and receptor signaling. However, it is unclear if the functional impairment is caused by the change in primary amino acid sequence or loss of glycosylation.

Reproduction of the $CSF2RA^{G174R}$ abnormality

To reproduce the GM-CSF receptor signaling defect identified in this family, plasmids expressing *CSF2RB* and either $CSF2RA^{G174R}$ or $CSF2RA^{WT}$ were cotransfected into 293 cells. Western blotting showed receptor proteins of the expected size from $CSF2RA^{WT}$ and smaller molecular forms from $CSF2RA^{G174R}$ (Fig. 4 A), which is similar to results for primary leukocytes (Fig. 2 B). Treatment of transduced cell lysates with Peptide: N-Glycosidase F, an amidase that cleaves between the innermost GlcNAc and asparagine residues of high mannose oligosaccharides (3), resulted in a similar electrophoretic pattern for normal and G174R GM-CSF-Rα. This confirmed the G174R mutation alters N-linked glycosylation (Fig. 4 A) by disrupting a functional N-linked glycosylation site and that glycosylation is responsible for the smaller molecular forms from this allele. GM-CSF-Rβ was expressed in *CSF2RB*-transfected cells but was undetectable in nontransfected cells (unpublished data). GM-CSF binding studies demonstrated that cells expressing $CSF2RA^{WT}$ and *CSF2RB* rapidly bound GM-CSF and removed it from the media, whereas cells expressing $CSF2RA^{G174R}$ and *CSF2RB* or *CSF2RB* alone

balanced hybridization to patient and control DNA are shown as clear boxes (A and D), whereas those showing an unbalanced hybridization representing sequences deleted in the patient are shown in black. High-resolution SNP analysis revealed that the deletion (red bar) extended from 1,308,324 to 2,881,011 bp. Sequence analysis (A) and PCR quantification of *CSF2RA* exon 7 (Fig. S4, available at http://www.jem.org/cgi/content/full/jem.20080990/DC1) demonstrated that the deletion included *CSF2RA* exon 7. The chromosomal location of the *CSF2RA* gene (1,347,701–1,388,827 bp) is indicated. (F) Pedigree of the family deduced from sequencing and *CSF2RA* allelic copy number determination experiments. The index case is indicated (arrow).

did not clear GM-CSF (Fig. 4 B). Cotransfection of *CSF2RB* together with *CSF2RA*^{WT}, but not with *CSF2RA*^{G174R}, resulted in expression of functional GM-CSF receptors as demonstrated by GM-CSF–dependent phosphorylation of STAT5 only with the former combination (Fig. 4 C). Incubation of *CSF2RA*^{G174R}/*CSF2RB*-transduced cells with higher concentrations of GM-CSF in the range of those observed in the index patient gave results similar to those obtained with primary leukocytes and clearly demonstrated a modest dose-dependent increase in STAT5 phosphorylation, which is consistent with a partial rescue of the signaling abnormality (Fig. 4 D).

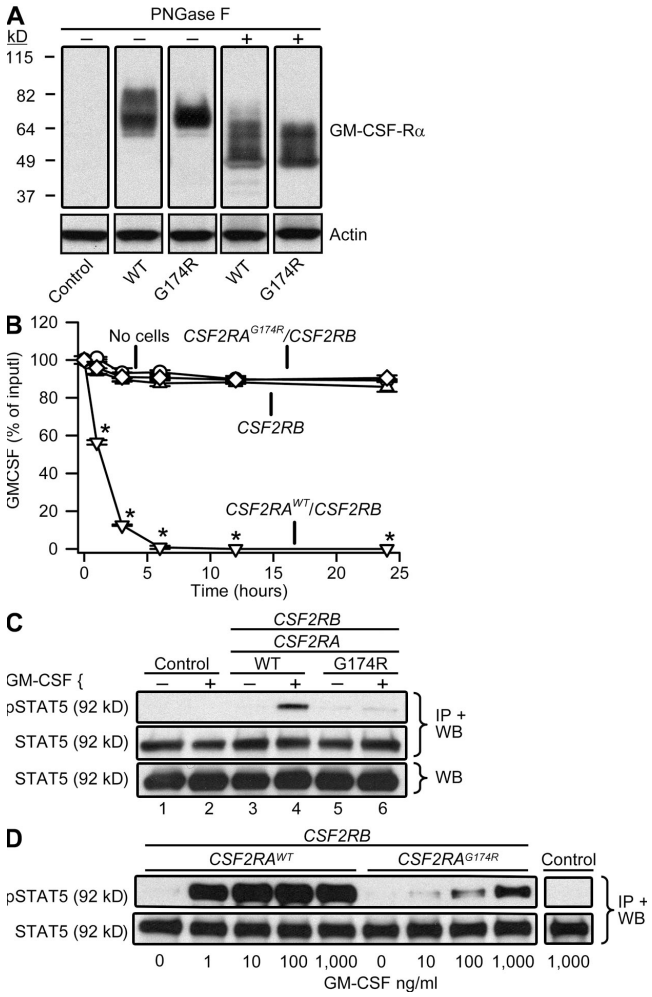

Figure 4. Reproduction of the *CSF2RA*^{G174R} gene defect. (A) Western blots of nontransfected 293 cell lysates (control) or lysates of cells transfected with plasmids expressing *CSF2RB* and either *CSF2RA*^{WT} (WT) or *CSF2RA*^{G174R} (G174R), followed by incubation with (+) or without (−) Peptide: N-Glycosidase F (PNGase F) and detection with antibodies against GM-CSF-Rα or actin. (B) Evaluation of cell-mediated binding and removal of exogenous GM-CSF from the culture media. Asterisks indicate significant differences in levels of GM-CSF in media from cells expressing *CSF2RA*^{WT}/*CSF2RB* compared with cells expressing *CSF2RA*^{G174R}/*CSF2RB*, *CSF2RB* alone or media without cells. Error bars show the means ± SE. (C) Evaluation of GM-CSF–stimulated phosphorylation of STAT5 in 293 cells transfected as described in A and incubated for 15 min in the absence (−) or presence (+) of 10 ng/ml GM-CSF. Lysates were evaluated by Western blotting (WB) to detect total STAT5 (STAT5) or were immunoprecipitated with anti-STAT5 antibody and then evaluated by Western blotting (IP + WB) to detect total STAT5 or phosphorylated STAT5 (pSTAT5). (D) Similar to C, except that increased concentrations of GM-CSF were used for evaluate GM-CSF receptor function.

Clinical relevance of the *CSF2RA*^{G174R} mutation

Our findings demonstrate that familial primary PAP in humans is caused by compound heterozygous abnormalities of *CSF2RA*, including loss of heterozygosity and a function-altering point mutation that severely reduces GM-CSF receptor signaling. These are the first results to demonstrate familial primary PAP in humans and that GM-CSF-Rα is critical for surfactant homeostasis. They extend previous findings that PAP is caused by the absence of GM-CSF or GM-CSF-Rβ in mice (4–6) or is specifically associated with the presence of neutralizing GM-CSF autoantibodies or a reduction in alveolar macrophage numbers or function in humans (9, 10). The allelic frequency of these mutations has not been determined but may be rare given that autoantibodies against GM-CSF account for most individuals with PAP.

Both affected siblings had impaired pulmonary function and failure to thrive, supporting the conclusion that prolonged respiratory insufficiency in children retards growth. Important to this conclusion is the observation that Xp22.33 deletion did not include the *SHOX* (*short stature homeobox*) gene, the deletion of which impairs growth (28). Further, heterozygous loss of *CSF2RA* in the mother did not impair growth. Early results suggest that whole lung lavage therapy was followed by an increase in growth acceleration in the index patient.

This study highlights the usefulness of several novel biomarkers in the diagnostic evaluation of PAP. The combination of a negative GM-CSF autoantibody test (29) and an abnormal CD11b stimulation index (24) predicted the GM-CSF receptor dysfunction, which was confirmed by the lack of GM-CSF binding and defective GM-CSF receptor signaling. GM-CSF levels were increased in lung lavage from the patient and, in serum from the patient and her sister, compared with family members and healthy controls. Because primary PAP is presumed to be caused by a defect in GM-CSF regulation of alveolar macrophage surfactant catabolism (9, 10), an elevated serum GM-CSF level may be useful as a biomarker to distinguish primary PAP caused by GM-CSF autoantibodies (90% of all cases of PAP) (9, 10, 13, 30) from PAP caused by GM-CSF receptor dysfunction (this study; references 14–16) and PAP caused by GM-CSF deficiency (4, 5) (not yet reported in humans). Finally, an increased serum SP-D level predicted the occurrence of PAP in the sister, which was confirmed by subsequent clinical and radiographical evaluation.

The slow progression and differences in severity of the lung disease between affected siblings with the same *CSF2RA* mutations and GM-CSF-Rα dysfunction indicates that penetrance is important in familial PAP because of GM-CSF receptor defects. The increased levels of GM-CSF likely reflect impaired clearance but are also consistent with interruption of a

negative-feedback regulatory loop. Results strongly suggest that the high levels of pulmonary GM-CSF present in epithelial lining fluid result in a reduced but not abrogated receptor signaling and provide a molecular explanation the slow progression of PAP in both affected siblings. It is currently unclear if the level of increased pulmonary GM-CSF correlates with disease severity. They also suggest that aerosolized delivery of GM-CSF to the lungs may be therapeutic because this approach could theoretically achieve pulmonary GM-CSF levels several thousand–fold higher than endogenous levels measured in the patient and 20-fold higher than levels that appeared to completely restore GM-CSF receptor signaling in the transfection experiments. BM transplantation and *CSF2RA* gene transfer represent other potentially therapeutic approaches.

The identification of mild PAP in the older sister provides a unique and important opportunity to observe PAP at a very early stage of disease development. Finally, this case exemplifies the utility of a collaborative approach to the diagnosis and treatment of individuals with very rare diseases involving geographically disparate clinical centers and the benefit derived from integrating basic science, clinical medicine, and translational research.

MATERIALS AND METHODS

Participants. The institutional review board of the Cincinnati Children's Hospital Medical Center approved the study, and all participants gave written informed consent or assent. Detailed case histories and laboratory data for the participants are included in the supplemental text (available at http://www.jem.org/cgi/content/full/jem.20080990/DC1).

GM-CSF receptor structure and function. GM-CSF receptors were evaluated by flow cytometry using antibodies recognizing GM-CSF-Rα (BD) or β (Santa Cruz Biotechnology, Inc.) and by Western blotting (7) with chain-specific antibodies (Santa Cruz Biotechnology, Inc.). The effects of glycosylation on GM-CSF-Rα were evaluated by incubating cell lysates with PNGase F (New England Biolabs, Inc.) (3). Actin was measured as a loading control using anti-actin antibodies (Santa Cruz Biotechnology, Inc.). To evaluate receptor-mediated clearance of GM-CSF, Ficoll-purified blood leukocytes or 293 cells (American Type Culture Collection) were cultured in DMEM containing 10% fetal bovine serum and human GM-CSF (Leukine; Bayer) at 1 ng/ml. At subsequent times, GM-CSF was measured in the culture medium by ELISA (R&D Systems) (24). To evaluate GM-CSF receptor signaling, heparinized blood was incubated with or without 10 ng/ml of human GM-CSF Leukine for 15 min. After lysing RBC, leukocytes were evaluated by Western blotting (24) using anti–human STAT5 (Santa Cruz Biotechnology, Inc.) and anti–phospho-STAT5 (Millipore) antibodies. The CD11b stimulation index was measured as previously described (24).

ELISA. SP-D, GM-CSF, MCP-1 (monocyte chemotactic protein-1), M-CSF, and urea were measured using commercial ELISA kits (BioVendor, R&D Systems, BD, R&D Systems, and BioAssay Systems, respectively) (24). The concentration of cytokines in epithelial lining fluid of the lungs was estimated by multiplying the concentration in lavage fluid by the ratio of urea concentrations in serum and lavage fluid (26).

Genetic analysis. Genomic DNA or total mRNA was purified from blood leukocytes with commercially available kits (QIAGEN). The PCR was used to generate products spanning exons and flanking intronic sequences (genomic DNA) or the coding sequences and 5′ and 3′ flanking untranslated sequences (mRNA) of the *CSF2RA* and *CSF2RB* genes, which were then analyzed by direct sequencing. The resulting sequences were compared with published sequences (from GenBank/EMBL/DDBJ under accession nos. NM_006140.3 and BC070085, respectively). The relative copy number of *CSF2RA* and *CSF2RB* genes among family members and a healthy control was measured by amplification of genomic DNA using PCR with gene-specific oligonucleotides followed by analysis of products by electrophoresis on 2% agarose gels. Experimental methods for measuring gene copy number, evaluating the genes encoding SP-B, SP-C, and ABCA3 (19, 31) for function-altering mutations, cytogenetic analysis, CGH analysis, FISH, and high-resolution SNP array analysis (32) are described in the supplemental Materials and methods (available at http://www.jem.org/cgi/content/full/jem.20080990/DC1).

Reproduction of the GM-CSF receptor defect. The methods used to clone and express mRNA transcripts encoding GM-CSF-Rα and β chains in cultured cells and evaluate protein glycosylation are described in the supplemental Materials and methods.

Statistical analysis. Numeric data are presented as means ± SE. Statistical comparisons were made with Student's *t* test for two-group comparisons and with one-way analysis of variance with posthoc analysis according to the Holm-Sidak method for multiple-group comparisons. P-values of <0.05 were considered to indicate statistical significance.

Online supplemental material. Fig. S1 shows normalized growth curves for the index patient and her sister. Fig. S2 shows GM-CSF binding and clearance by blood leukocytes from affected and unaffected family members and control. Fig. S3 shows increased pulmonary GM-CSF levels in GM-CSF receptor β chain (*Csf2rb*) KO mice. Fig. S4 shows evaluation of *CSF2RA* and CSF2FB gene copy number by PCR amplification. Fig. S5 shows karyotypes of high-resolution GTG-banded chromosomes. Fig. S6 shows evaluation of heterozygosity at the *CSF2RA* locus by FISH. Fig. S7 shows high-resolution SNP analysis. The supplemental text contains additional details regarding the case histories and clinical laboratory and other data cited throughout the text. Online supplemental material is available at http://www.jem.org/cgi/content/full/jem.20080990/DC1.

We thank Diana Koch, Diane Black, Paula Blair, and Ralph Stanley (Cincinnati Children's Hospital Medical Center) for excellent technical assistance, Dr. Denis McGraw (University of Cincinnati Medical Center) for performing bronchoalveolar lavage in healthy controls, Dr. Frank McCormack (University of Cincinnati College of Medicine) for helpful discussions, and Lauren Vannoy (Wake Forest University School of Medicine and the Translational Research Trials Office, Cincinnati Children's Hospital Medical) for clinical research coordination.

This work was supported in part by the grants from the National Center For Research Resources (RR019498 to B.C. Trapnell to support the Rare Lung Diseases Consortium) and the National Heart, Lung, and Blood Institute (HL085453 to B.C. Trapnell and HL085610 to J.A. Whitsett), and the Division of Pulmonary Biology at the Children's Hospital Medical Center.

The authors have no conflicting financial interests.

Submitted: 7 May 2008
Accepted: 22 September 2008

REFERENCES

1. Trapnell, B.C., and J.A. Whitsett. 2002. GM-CSF regulates pulmonary surfactant homeostasis and alveolar macrophage-mediated innate host defense. *Annu. Rev. Physiol.* 64:775–802.
2. Guthridge, M.A., J.A. Powell, E.F. Barry, F.C. Stomski, B.J. McClure, H. Ramshaw, F.A. Felquer, M. Dottore, D.T. Thomas, B. To, et al. 2006. Growth factor pleiotropy is controlled by a receptor Tyr/Ser motif that acts as a binary switch. *EMBO J.* 25:479–489.
3. Shibuya, K., S. Chiba, K. Miyagawa, T. Kitamura, K. Miyazono, and F. Takaku. 1991. Structural and functional analyses of glycosylation on the distinct molecules of human GM-CSF receptors. *Eur. J. Biochem.* 198:659–666.
4. Dranoff, G., A.D. Crawford, M. Sadelain, B. Ream, A. Rashid, R.T. Bronson, G.R. Dickersin, C.J. Bachurski, E.L. Mark, J.A. Whitsett,

et al. 1994. Involvement of granulocyte-macrophage colony-stimulating factor in pulmonary homeostasis. *Science*. 264:713–716.
5. Stanley, E., G.J. Lieschke, D. Grail, D. Metcalf, G. Hodgson, J.A. Gall, D.W. Maher, J. Cebon, V. Sinickas, and A.R. Dunn. 1994. Granulocyte/macrophage colony-stimulating factor-deficient mice show no major perturbation of hematopoiesis but develop a characteristic pulmonary pathology. *Proc. Natl. Acad. Sci. USA*. 91:5592–5596.
6. Robb, L., C.C. Drinkwater, D. Metcalf, R. Li, F. Kontgen, N.A. Nicola, and C.G. Begley. 1995. Hematopoietic and lung abnormalities in mice with a null mutation of the common beta subunit of the receptors for granulocyte-macrophage colony-stimulating factor and interleukins 3 and 5. *Proc. Natl. Acad. Sci. USA*. 92:9565–9569.
7. Shibata, Y., P.Y. Berclaz, Z.C. Chroneos, M. Yoshida, J.A. Whitsett, and B.C. Trapnell. 2001. GM-CSF regulates alveolar macrophage differentiation and innate immunity in the lung through PU.1. *Immunity*. 15:557–567.
8. Ikegami, M., T. Ueda, W. Hull, J.A. Whitsett, R.C. Mulligan, G. Dranoff, and A.H. Jobe. 1996. Surfactant metabolism in transgenic mice after granulocyte macrophage-colony stimulating factor ablation. *Am. J. Physiol.* 270:L650–L658.
9. Seymour, J.F., and J.J. Presneill. 2002. Pulmonary alveolar proteinosis: progress in the first 44 years. *Am. J. Respir. Crit. Care Med*. 166:215–235.
10. Trapnell, B.C., J.A. Whitsett, and K. Nakata. 2003. Pulmonary alveolar proteinosis. *N. Engl. J. Med*. 349:2527–2539.
11. Presneill, J.J., K. Nakata, Y. Inoue, and J.F. Seymour. 2004. Pulmonary alveolar proteinosis. *Clin. Chest Med*. 25:593–613.
12. Seymour, J.F., and J.J. Presneill. 2004. Pulmonary alveolar proteinosis. What is the role of GM-CSF in disease pathogenesis and treatment? *Treat. Respir. Med*. 3:229–234.
13. Inoue, Y., B.C. Trapnell, R. Tazawa, T. Arai, T. Takada, N. Hizawa, Y. Kasahara, K. Tatsumi, M. Hojo, T. Ichiwata, et al. 2008. Characteristics of a large cohort of patients with autoimmune pulmonary alveolar proteinosis in Japan. *Am. J. Respir. Crit. Care Med*. 177:752–762.
14. Dirksen, U., R. Nishinakamura, P. Groneck, U. Hattenhorst, L. Nogee, R. Murray, and S. Burdach. 1997. Human pulmonary alveolar proteinosis associated with a defect in GM-CSF/IL-3/IL-5 receptor common beta chain expression. *J. Clin. Invest*. 100:2211–2217.
15. Dirksen, U., U. Hattenhorst, P. Schneider, H. Schroten, U. Gobel, A. Bocking, K.M. Muller, R. Murray, and S. Burdach. 1998. Defective expression of granulocyte-macrophage colony-stimulating factor/interleukin-3/interleukin-5 receptor common beta chain in children with acute myeloid leukemia associated with respiratory failure. *Blood*. 92:1097–1103.
16. Bewig, B., X.D. Wang, D. Kirsten, K. Dalhoff, and H. Schafer. 2000. GM-CSF and GM-CSF beta c receptor in adult patients with pulmonary alveolar proteinosis. *Eur. Respir. J.* 15:350–357.
17. Nogee, L.M., D.E. de Mello, L.P. Dehner, and H.R. Colten. 1993. Brief report: deficiency of pulmonary surfactant protein B in congenital alveolar proteinosis. *N. Engl. J. Med*. 328:406–410.
18. Nogee, L.M., A.E. Dunbar III, S.E. Wert, F. Askin, A. Hamvas, and J.A. Whitsett. 2001. A mutation in the surfactant protein C gene associated with familial interstitial lung disease. *N. Engl. J. Med*. 344:573–579.
19. Shulenin, S., L.M. Nogee, T. Annilo, S.E. Wert, J.A. Whitsett, and M. Dean. 2004. ABCA3 gene mutations in newborns with fatal surfactant deficiency. *N. Engl. J. Med*. 350:1296–1303.
20. Whitsett, J.A., S.E. Wert, and B.C. Trapnell. 2004. Genetic disorders influencing lung formation and function at birth. *Hum. Mol. Genet*. 13:R207–R215.
21. Uchida, K., K. Nakata, B.C. Trapnell, T. Terakawa, E. Hamano, A. Mikami, I. Matsushita, J.F. Seymour, M. Oh-Eda, I. Ishige, et al. 2004. High-affinity autoantibodies specifically eliminate granulocyte-macrophage colony-stimulating factor activity in the lungs of patients with idiopathic pulmonary alveolar proteinosis. *Blood*. 103:1089–1098.
22. Iyonaga, K., M. Suga, T. Yamamoto, H. Ichiyasu, H. Miyakawa, and M. Ando. 1999. Elevated bronchoalveolar concentrations of MCP-1 in patients with pulmonary alveolar proteinosis. *Eur. Respir. J.* 14:383–389.
23. Paine, R. III, S.B. Morris, H. Jin, S.E. Wilcoxen, S.M. Phare, B.B. Moore, M.J. Coffey, and G.B. Toews. 2001. Impaired functional activity of alveolar macrophages from GM-CSF-deficient mice. *Am. J. Physiol. Lung Cell. Mol. Physiol*. 281:L1210–L1218.
24. Uchida, K., D.C. Beck, T. Yamamoto, P.Y. Berclaz, S. Abe, M.K. Staudt, B.C. Carey, M.D. Filippi, S.E. Wert, L.A. Denson, et al. 2007. GM-CSF autoantibodies and neutrophil dysfunction in pulmonary alveolar proteinosis. *N. Engl. J. Med*. 356:567–579.
25. Seymour, J.F., I.R. Doyle, K. Nakata, J.J. Presneill, O.D. Schoch, E. Hamano, K. Uchida, R. Fisher, and A.R. Dunn. 2003. Relationship of anti-GM-CSF antibody concentration, surfactant protein A and B levels, and serum LDH to pulmonary parameters and response to GM-CSF therapy in patients with idiopathic alveolar proteinosis. *Thorax*. 58:252–257.
26. Rennard, S.I., G. Basset, D. Lecossier, K.M. O'Donnell, P. Pinkston, P.G. Martin, and R.G. Crystal. 1986. Estimation of volume of epithelial lining fluid recovered by lavage using urea as marker of dilution. *J. Appl. Physiol*. 60:532–538.
27. Ding, D.X., J.C. Vera, M.L. Heaney, and D.W. Golde. 1995. N-glycosylation of the human granulocyte-macrophage colony-stimulating factor receptor alpha subunit is essential for ligand binding and signal transduction. *J. Biol. Chem*. 270:24580–24584.
28. Shears, D.J., H.J. Vassal, F.R. Goodman, R.W. Palmer, W. Reardon, A. Superti-Furga, P.J. Scambler, and R.M. Winter. 1998. Mutation and deletion of the pseudoautosomal gene SHOX cause Leri-Weill dyschondrosteosis. *Nat. Genet*. 19:70–73.
29. Kitamura, T., K. Uchida, N. Tanaka, T. Tsuchiya, J. Watanabe, Y. Yamada, K. Hanaoka, J.F. Seymour, O.D. Schoch, I. Doyle, et al. 2000. Serological diagnosis of idiopathic pulmonary alveolar proteinosis. *Am. J. Respir. Crit. Care Med*. 162:658–662.
30. Kitamura, T., N. Tanaka, J. Watanabe, K. Uchida, S. Kanegasaki, Y. Yamada, and K. Nakata. 1999. Idiopathic pulmonary alveolar proteinosis as an autoimmune disease with neutralizing antibody against granulocyte/macrophage colony-stimulating factor. *J. Exp. Med*. 190:875–880.
31. Nogee, L.M. 2004. Alterations in SP-B and SP-C expression in neonatal lung disease. *Annu. Rev. Physiol*. 66:601–623.
32. Redon, R., S. Ishikawa, K.R. Fitch, L. Feuk, G.H. Perry, T.D. Andrews, H. Fiegler, M.H. Shapero, A.R. Carson, W. Chen, et al. 2006. Global variation in copy number in the human genome. *Nature*. 444:444–454.

Suzuki et al., http://www.jem.org/cgi/content/full/jem.20080990/DC1

PARTICIPANTS

Patient. The index case was a 6-yr-old girl who was admitted to the hospital in July, 2007 when a chest radiograph revealed bilateral diffuse alveolar infiltrates. She was the product of a normal gestation and delivery and had reached developmental milestones as expected. At birth, she weighed 3.64 kg and was 19.5 cm in length (both at the 50th percentile); however, by 6–9 mo weight gain slowed and by 2–3 yr height acceleration slowed (Fig. S1 A). On admission, both her weight (13.6 kg) and height (103.5 cm) were below the third percentile for her age. She was noted by her mother to avoid swimming underwater at 3–4 yr of age, refusing to hold her breath. By 4–5 yr of age, she had developed dyspnea of insidious onset, first with exercise and then at rest, and finally was noted to "pant" in her sleep. There was no history of cough, fever, chest pain, lymphadenopathy, pneumonia or serious infection, pulmonary or other disease, environmental exposures, or drug use. There was no family history of lung disease in children or unexplained deaths at an early age. On examination, the respiratory rate was 60 per minute, blood pressure was 88/30 mm Hg, and pulse was 106. Pulmonary auscultation revealed mild crackles during deep inspiration, but the remainder of the exam was otherwise unremarkable.

The white blood cell count was 5.9×10^3/ml with normal cytometric indices, the RBC count was 4.9 million/mm^3, the hemoglobin was 13.9 g/deciliter, and the hematocrit was 41.1%. The levels of serum IgG, IgA, and IgM were mildly elevated (995, 150, and 181 g/deciliter, respectively) and IgE was 6.2 g/deciliter. Pulmonary function testing revealed a pattern of severe restriction with a forced vital capacity (FVC) that was 44% of that predicted, forced expiratory volume in one second (FEV1) 44% that of predicted, and a FEV1/FVC ratio 116% of that predicted. Oxygen saturation was 88% while breathing room air and dropped when talking or walking a short distance. A chest radiograph showed diffuse patchy alveolar infiltrates throughout both lung fields (Fig. 1 A, top). Bronchoscopic examination of the airways was unremarkable. Cytological examination of the bronchoalveolar lavage fluid demonstrated the presence of lipoproteinaceous material. A GMS stain was negative and cultures were negative for bacterial, fungal, or microbial pathogens. The lung lavage fluid from the patient contained increased levels of MCP-1 (25,085 pg/ml) and M-CSF (8,313 pg/ml) compared with lung lavage from five healthy controls (23 ± 8.2 and 35.0 ± 3.6 pg/ml, respectively). A high-resolution computed tomogram (HRCT) of the chest showed extensive ground glass opacification and increased interlobular thickening throughout both lung fields, suggesting the diagnosis of PAP (Fig. 1 A, bottom). Histopathological examination of lung parenchyma obtained by open lung biopsy showed alveolar filling with good preservation of alveolar wall integrity and the presence of focal areas of lymphocytosis (Fig. 2 B). Immunohistochemical staining demonstrated the presence of SP-A, mature SP-B, and SP-D within the endoalveolar space and pro–SP-C and ABCA3 within alveolar type II epithelial cells (Fig. 1 B). A serum GM-CSF antibody test was negative on two occasions. The urine did not contain detectable amino acids. No sequence deviations were detected in the coding exons and intron–exon boundaries of the genes encoding SPs B and C and ABCA3 (1, 2).

The patient was transferred to Cincinnati Children's Hospital in October, 2007 and underwent whole lung lavage therapy, which resulted in marked symptomatic improvement (Fig. 1 C). 4 mo later, the oxygen saturation was 98% on room air, and pulmonary function testing revealed an FVC that was 69% of that predicted, an FEV1 of 61% that predicted, and an FEV1/FVC ratio of 116% that predicted. The weight had increased to 16 kg and the height to 107.5 cm. Exercise tolerance had markedly improved and the patient resumed more normal daily activities.

Sister. The sister of the index patient was 8 yr old in February, 2008 when first evaluated after a negative GM-CSF autoantibody test and an abnormal CD11b stimulation index test suggested that an inherited GM-CSF receptor defect may be present in the index case (3). She was the product of a normal gestation and delivery and had reached developmental milestones as expected. At birth, her weight and length were 3.64 kg and 20 cm (both at the 50th percentile) and at the time of evaluation were 22.7 kg and 122 cm, respectively (both at the 10th percentile for age; Fig. S1B). She had been considered by her family to have been healthy all her life with no history of lung disease or major illnesses. On examination, the respiratory rate was 32 per minute, the pulse was 82 per minute, and blood pressure was 104/62 mm Hg and was otherwise unremarkable. Pulmonary function testing demonstrated an FVC that was 88% of that predicted, FEV1 that was 90% of that predicted, a FEV1/FVC ratio that was 92% of that predicted, and a diffusion capacity for carbon dioxide (DLCO) that was 57% of that predicted. Oxygen saturation was 97% while breathing room air. An HRCT of the chest revealed mild patchy ground glass opacities throughout both lungs, which is consistent with the diagnosis of PAP (Fig. 1 E). The severe reduction in DLCO and failure to thrive suggest that the lung abnormalities are more extensive than indicated by the chest HRCT; i.e., scattered ground glass opacifications involving geographically distributed secondary pulmonary lobules. Rather, these results suggest that a thickened alveolar surfactant layer may be present throughout the alveolar surface but is not well visualized by the radiographical technique used.

Father. The father of the index patient was 49 yr old at the time of evaluation in February, 2008. His height was 185.4 cm (85th percentile for his age). He was a lifelong nonsmoker with no history of pulmonary or other major medical illness.

Mother. The mother of the index patient was 48 yr old at the time of evaluation in February, 2008. Her height was 165 cm

(65th percentile for her age). She was a lifelong nonsmoker with no history of pulmonary or other major medical illness.

Patients with autoimmune PAP. 12 individuals with autoimmune PAP are reported as disease controls, all of whom had the typical clinical, physiological, and radiographical features of the disease at the time of evaluation. The detailed case histories and diagnostic criteria of each have been reported previously (3). The group included three pediatric and nine adult patients. The mean ± SE GM-CSF autoantibody titer was 324.3 ± 66 μg/ml and was similar in adult and pediatric cases (365 ± 74 and 202 ± 141 μg/ml, respectively; P = 0.308).

Healthy controls. Volunteers were enrolled in the study as healthy controls. This control group included 67 individuals, 61 of whom were previously reported as part of another study (3). The mean ± SE age was 30 ± 6 yr. All were disease-free healthy individuals without a history of major illness and all were symptom-free at the time of enrollment in the study. None were current smokers.

MATERIALS AND METHODS

Lung histopathology and immunostaining

A formalin-fixed paraffin-embedded open lung biopsy tissue sample was received for evaluation. 5-μm-thick sections were cut on a rotary microtome and loaded onto polylysine-coated slides. Hematoxylin and eosin–stained sections were prepared using routine methods. Immunohistochemistry was performed as described previously (4, 5) using rabbit polyclonal antisera raised against SP-A, SP-B, pro–SP-C, and SP-D, a mouse monoclonal antibody generated to ABCA3 as primary antibodies and biotinylated secondary antibodies (Vector Laboratories), and an avidin-biotin–horseradish peroxidase detection system (ABC reagent; Vector Laboratories). The enzymatic reaction product was enhanced using Ni-DAB and Tris cobalt to give a black precipitate, and the sections were counterstained with Nuclear Fast Red.

GM-CSF clearance assay

To evaluate receptor-mediated binding of GM-CSF, heparinized blood was obtained by phlebotomy and mononuclear cells were isolated on Ficoll gradients, followed by RBC lysis as previously described (3). Primary mononuclear cells or transfected 293 cells (see Construction of vectors and transfection) were seeded into culture dishes at 1 × 106 cells per dish in DMEM containing 10% bovine calf serum. Human GM-CSF (Leukine; Bayer) was added at a concentration of 1 ng/ml. At subsequent times, GM-CSF was measured in aliquots of the culture medium by ELISA (R&D Systems). The results were expressed as a percentage of initial GM-CSF concentration.

Nucleotide sequence analysis

The nucleotide sequence of *CSF2RA* and *CSF2RB* transcripts and genomic DNA were determined by PCR-based methods in the Genetic Variation and Gene Discovery Core Facility at the Cincinnati Children's Hospital Medical Center. Genomic DNA was also evaluated for the presence of known function-altering mutations in the coding sequences and intron–exon boundaries of the genes encoding SP-B, SP-C, and ABCA3 as previously described (1, 2).

Measurement of gene copy number by PCR amplification

The relative copy number of *CSF2RA* and *CSF2RB* genes among family members and controls was determined using genomic DNA using PCR with the following gene-specific primers: 5′-AGGAG AAGGAGGGAGATCCG-3′, 5′-CACGTG-GCCTCAGTTACACAG-3′ (*CSF2RA*); 5′-ACAG AGCCAGGCATGTGGT-3′, and 5′- CGACAAAACTCTG-GCAGGG-3′ (*CSF2RB*). Amplification conditions were as follows: 94°C for 5 min; 94°C for 30 s, 58°C for 30 s, and 72°C for 45 s (30 cycles); and 72°C for 7 min. PCR-generated products were then evaluated by electrophoresis on 2% agarose gels.

Cytogenetics

Chromosome analysis was performed on cells isolated from peripheral blood according to standard cytogenetic techniques.

Comparative genomic hybridization

Comparative genomic hybridization analysis was performed with genomic DNA isolated from each family member using the SignatureSelect V2 microarray chips (Signature Genomic Laboratories, LLC) and a fluorescence dye reversal assay (6). Microarray chips were processed according to the manufacturer's protocol. Genomic DNA were evaluated with a same-sex reference DNA (patient) or an opposite sex reference DNA (mother and sister) and data analysis was performed using the Genoglyphix software (Signature Genomic Laboratories, LLC).

Fluorescence in situ hybridization

FISH analysis was performed under routine clinical laboratory protocols with the CTD-3047L21 hybridization probe, which identifies the pseudoautosomal region of X and Y chromosomes, Xp22.33 and Yp11.32, respectively. Slides were analyzed with a fluorescent microscope (Carl Zeiss, Inc.) with CytoVision v3.7 software (Applied Imaging). 8–10 metaphases and 25 interphase cells were evaluated in each FISH study.

High-resolution single-nucleotide polymorphism analysis

Blood was obtained from the patient, her sister, and parents, and genomic DNA was isolated using a commercial kit (QIAGEN) according to the manufacturer's instructions. Samples of genomic DNA (750 ng) from each subject were prepared for microarray analysis using the Infinium Assay (Illumina Inc.) according to the manufacturer's protocol. Microarray analysis was performed using the HumanCNV370-duo DNA Analysis BeadChip platform (Illumina Inc.). This chip contains ~370,404 markers, including SNP and copy number variation content. Data were analyzed using the BeadStudio v3.1 analysis software (Illumina Inc.).

Construction of vectors and transfection

PBMC RNA from the index patient and a healthy control was purified and converted to cDNA as described in the Ma-

terials and methods section Genetic analysis. The nucleotide sequence for the entire protein coding sequence of *CSF2RA* was generated from cDNA transcripts by PCR amplification using gene-specific primers and subcloned into pSC-A (Agilent Technologies). After confirming the nucleotide sequence, a restriction fragment containing the entire coding region of *CSF2RA* from the control (*CSF2RA*WT) or the index patient (*CSF2RA*G174R) were inserted individually into a plasmid (MIEG3) permitting expression in mammalian cells (7). The cDNA encoding *CSF2RB* was obtained (IART98-E2; Geneservice) and inserted into another plasmid (MSCV2.1) permitting expression in mammalian cells (8). Expression plasmids carrying *CSF2RB*WT and either *CSF2RA*G174R or *CSF2RA*WT were cotransfected into human embryonic kidney epithelial cells (HEK 293 cells; American Type Culture Collection) using Lipofectamine2000 (Invitrogen) according to the manufacturer's instructions. After 48 h, cells were evaluated for (1) expression of GM-CSF receptor proteins by Western blotting (2), GM-CSF binding, and clearance by culturing with exogenous GM-CSF (see GM-CSF clearance assay) or (3) GM-CSF receptor signaling by evaluation of GM-CSF–dependent phosphorylation of STAT5 (see STAT5).

Western blotting

GM-CSF-Rα.

GM-CSF-Rα was evaluated in blood leukocytes or transfected cells as follows. Leukocytes from 1 ml of blood (evaluated within 1 h of phlebotomy and subjected to RBC lysis) or 1×10^6 transfected 293 cells were lysed in 200 μl RIPA buffer (0.05 M Tris-HCl, pH 8, 0.15 M NaCl [Tris-buffered saline (TBS)], 1% vol/vol nonidet P-40, 0.5% wt/vol sodium deoxycholate, 0.1% wt/vol SDS, 0.004% wt/vol sodium azide) containing 2% vol/vol proteinase inhibitor cocktail, 1% vol/vol phenyl-methyl-sulfonyl-fluoride (PMSF), and 1% vol/volsodium orthovanadate (Santa Cruz Biotechnology, Inc.) as directed by the manufacturer. Samples were kept on ice for 30 min and then centrifuged (9000 *g* at 4°C for 15 min) to remove insoluble debris. Samples were mixed with equal volume of sample buffer and boiled. The lysate was then fractionated on SDS-PAGE gels (4–12% Tris Glycine gel; Invitrogen) under reducing conditions and proteins were transferred to PVDF membranes by electroblotting. Membranes were incubated in blotting solution (TBS, 5% [wt/vol] dry milk, and 0.1% [vol/vol] Tween 20) at 4°C, overnight to block nonspecific binding. Mouse antihuman GM-CSF-Rα antibody (diluted 1:500; Santa Cruz Biotechnology, Inc.) was then added and incubations were continued at room temperature for 2 h. After washing in TBS and 0.1% (vol/vol) Tween 20, membranes were incubated at room temperature for 1 h in blotting solution containing donkey anti–rabbit IgG. After washing in blotting solution, membranes were incubated with ECL-Plus (GE Healthcare) to visualize immunostained proteins as directed by the manufacturer. This procedure was used for measuring actin in the same samples with anti-Actin antibody (diluted 1:1,000; Santa Cruz Biotechnology, Inc.).

STAT5.

GM-CSF receptor signaling was evaluated in blood leukocytes or transfected cells as described for GM-CSF-Rα with the following modifications. 1 ml of blood (evaluated within 1 h of phlebotomy) or 1×10^6 transfected 293 cells (in DMEM containing 10% bovine calf serum) were incubated in the absence or presence of human GM-CSF (Leukine; 1, 10, 100, and 1,000 ng/ml) for 15 min at 37°C. After RBC lysis (whole blood) and washing with PBS (both leukocytes and 293 cells), cell lysates were prepared and evaluated as in GM-CSF-Rα, except that for transfected 293 cell lysates and cells exposed to high GM-CSF concentrations, immunoprecipitation was performed at 4°C overnight using ProteinA/G Agarose (Santa Cruz Biotechnology, Inc.) and anti-STAT5 antibody or control rabbit IgG (Santa Cruz Biotechnology, Inc.). Anti-STAT5 antibody (diluted 1:500; Santa Cruz Biotechnology, Inc.) or anti–phospho-STAT5 (diluted 1:500; Millipore) were used for primary antibodies for Western blotting.

Evaluation of CSF2RA glycosylation

Expression plasmids carrying either *CSF2RA*G174R or *CSF2RA*WT were transfected into 1×10^6 HEK 293 cells as described in Construction of vectors and transfection. After 48 h, cells were lysed in 200 μl RIPA buffer containing proteinase inhibitor cocktail, PMSF, sodium orthovanadate (Santa Cruz Biotechnology, Inc.). Samples were kept on ice for 30 min and then centrifuged at 9,000 *g* at 4°C for 15 min to remove insoluble debris. Nine μl of lysate was treated with PNGase F (New England Biolabs, Inc.) at 37°C for 30 min according to the manufacturer's protocol and then evaluated by Western blotting as in GM-CS-Rα.

Measurement of cytokine concentration in lung epithelial lining fluid recovered by bronchoalveolar lavage

The volume of epithelial lining fluid (ELF) recovered in lung lavage fluid was estimated using the urea dilution method described by Rennard et al. (9). In brief, the concentration of urea in the lung lavage fluid and serum were measured by ELISA. The volume of ELF (in milliliters) was calculated as the volume of lavage fluid in milliliters multiplied by the concentration of urea in lavage fluid in milligrams per milliliters divided by the concentration of urea in plasma in milligrams per milliliters. The concentration of cytokines in ELF was estimated by multiplying their concentration in lavage fluid (measured by ELISA) by the ratio of the lavage fluid in milliliters to ELF volume in milliliters.

REFERENCES

1. Nogee, L.M. 2004. Alterations in SP-B and SP-C expression in neonatal lung disease. *Annu. Rev. Physiol.* 66:601–623.
2. Shulenin, S., L.M. Nogee, T. Annilo, S.E. Wert, J.A. Whitsett, and M. Dean. 2004. ABCA3 gene mutations in newborns with fatal surfactant deficiency. *N. Engl. J. Med.* 350:1296–1303.
3. Uchida, K., D.C. Beck, T. Yamamoto, P.Y. Berclaz, S. Abe, M.K. Staudt, B.C. Carey, M.D. Filippi, S.E. Wert, L.A. Denson, et al. 2007. GM-CSF autoantibodies and neutrophil dysfunction in pulmonary alveolar proteinosis. *N. Engl. J. Med.* 356:567–579.

4. Nogee, L.M., S.E. Wert, S.A. Proffit, W.M. Hull, and J.A. Whitsett. 2000. Allelic heterogeneity in hereditary surfactant protein B (SP-B) deficiency. *Am. J. Respir. Crit. Care Med.* 161:973–981.
5. Stahlman, M.T., V. Besnard, S.E. Wert, T.E. Weaver, S. Dingle, Y. Xu, K. von Zychlin, S.J. Olson, and J.A. Whitsett. 2007. Expression of ABCA3 in developing lung and other tissues. *J. Histochem. Cytochem.* 55:71–83.
6. Bejjani, B.A., and L.G. Shaffer. 2006. Application of array-based comparative genomic hybridization to clinical diagnostics. *J. Mol. Diagn.* 8:528–533.
7. Williams, D.A., W. Tao, F. Yang, C. Kim, Y. Gu, P. Mansfield, J.E. Levine, B. Petryniak, C.W. Derrow, C. Harris, et al. 2000. Dominant negative mutation of the hematopoieticspecific Rho GTPase, Rac2, is associated with a human phagocyte immunodeficiency. *Blood.* 96:1646–1654.
8. Hansen, W.K., W.A. Deutsch, A. Yacoub, Y. Xu, D.A. Williams, and M.R. Kelley. 1998. Creation of a fully functional human chimeric DNA repair protein. Combining O6- methylguanine DNA methyltransferase (MGMT) and AP endonuclease (APE/redox effector factor 1 (Ref 1)) DNA repair proteins. *J. Biol. Chem.* 273:756–762.
9. Rennard, S.I., G. Basset, D. Lecossier, K.M. O'Donnell, P. Pinkston, P.G. Martin, and R.G. Crystal. 1986. Estimation of volume of epithelial lining fluid recovered by lavage using urea as marker of dilution. *J. Appl. Physiol.* 60:532–538.